

# Recent Trends in Arctic Sea Ice and the Evolving Role of Atmospheric Circulation Forcing, 1979–2007

Clara Deser and Haiyan Teng

*National Center for Atmospheric Research, Boulder, Colorado, USA*

This study documents the evolving trends in Arctic sea ice extent and concentration during 1979–2007 and places them within the context of overlying changes in the atmospheric circulation. Results are based on 5-day running mean sea ice concentrations (SIC) from passive microwave measurements during January 1979 to October 2007. Arctic sea ice extent has retreated at all times of the year, with the largest declines ( $0.65 \times 10^6$  km<sup>2</sup> per decade, equivalent to 10% per decade in relative terms) from mid July to mid October. The pace of retreat has accelerated nearly threefold from the first half of the record to the second half, and the number of days with SIC less than 50% has increased by 19 since 1979. The spatial patterns of the SIC trends in the two halves of the record are distinctive, with regionally opposing trends in the first half and uniformly negative trends in the second half. In each season, these distinctive patterns correspond to the first two leading empirical orthogonal functions of SIC anomalies during 1979–2007. Atmospheric circulation trends and accompanying changes in wind-driven atmospheric thermal advection have contributed to thermodynamic forcing of the SIC trends in all seasons during the first half of the record and to those in fall and winter during the second half. Atmospheric circulation trends are weak over the record as a whole, suggesting that the long-term retreat of Arctic sea ice since 1979 in all seasons is due to factors other than wind-driven atmospheric thermal advection.

## 1. INTRODUCTION

The accelerating retreat of Arctic sea ice in recent decades, evident in all months of the year, is one of the most dramatic signals of climate change worldwide (see *Serreze et al.* [2007], *Meier et al.* [2007], and *Stroeve et al.* [2007] for recent overviews; ongoing updates on Arctic sea ice may be obtained from the National Snow and Ice Data Center (available at <http://nsidc.org>)). Although climate models

predict that Arctic sea ice will decline in response to atmospheric greenhouse gas increases [*Holland et al.*, 2006], the current pace of retreat at the end of the melt season is exceeding the models' forecasts by approximately a factor of 3 [*Stroeve et al.*, 2007]. Long-term records of summer sea ice extent within the central Arctic Ocean dating back to 1900 exhibit large multidecadal variations [*Polyakov et al.*, 2003], a factor which must be taken into account when interpreting the recent sea ice retreat.

The physical mechanisms underlying the Arctic sea ice decline are not fully understood but include dynamical processes related to changes in winds and ocean currents and thermodynamic processes involving changes in air temperature, radiative and turbulent energy fluxes, ocean heat storage, and ice-albedo feedback [*Serreze et al.*, 2007; *Stroeve and*

Arctic Sea Ice Decline: Observations, Projections, Mechanisms, and Implications  
Geophysical Monograph Series 180  
Copyright 2008 by the American Geophysical Union.  
10.1029/180GM03

Maslowski, 2008; Francis and Hunter, 2006, 2007; Shimada et al., 2006; Perovich et al., 2007]. A better understanding of these mechanisms and their relationship to increasing greenhouse gas concentrations is an important step for assessing future predictions of Arctic climate change.

Numerous studies indicate that the atmospheric circulation played an important role in driving Arctic sea ice declines from the 1960s to the early 1990s [e.g., Deser et al., 2000; Rigor et al., 2002; Hu et al., 2002; Rigor and Wallace, 2004; Rothrock and Zhang, 2005; Stroeve et al., 2007; Serreze and Francis, 2006; Ukita et al., 2007]. In particular, the declines during this period were due in part to a trend in the dominant pattern of wintertime atmospheric circulation variability over the high-latitude Northern Hemisphere known variously as the “North Atlantic Oscillation,” “Arctic Oscillation,” or “Northern Annular Mode” [Hurrell, 1995; Deser, 2000; Thompson and Wallace, 2000], collectively referred to hereinafter as the “NAM.” In particular, the anomalous cyclonic wind circulation associated with the upward trend in the winter NAM flushed old, thick ice out of the Arctic via Fram Strait, causing the winter ice pack to thin, which, in turn, preconditioned the summer ice pack for enhanced melt.

Since the early 1990s, however, the trend in the NAM has reversed sign, yet Arctic sea ice has continued to decline [Overland and Wang, 2005; Comiso, 2006; Serreze and Francis, 2006; Maslanik et al., 2007; Serreze et al., 2007; Stroeve and Maslowski, 2008]. This has led to speculation that the Arctic climate system has reached a “tipping point” whereby strong positive feedback mechanisms such as those associated with ice albedo and open water formation efficiency are accelerating the thinning and retreat of Arctic sea ice [e.g., Lindsay and Zhang, 2005; Holland et al., 2006]. These positive feedback mechanisms leave the ice pack more vulnerable to forcing from other processes, natural and anthropogenic. For example, enhanced downward longwave radiation associated with increases in air temperature, water vapor and cloudiness over the Arctic Ocean [Francis and Hunter, 2006] along with enhanced ocean heat transport into the Arctic [Polyakov et al., 2005; Shimada et al., 2006; Stroeve and Maslowski, 2008] and positive ice-albedo feedback [Perovich et al., 2007] have become dominant factors driving summer sea ice extent declines since the mid-to-late 1990s. There is also evidence that the winter atmospheric circulation has continued to affect the winter sea ice distribution since the mid-1990s [Comiso, 2006; Maslanik et al., 2007; Francis and Hunter, 2007].

The purpose of this study is to revisit the issue of Arctic sea ice trends from 1979 to present in the context of evolving atmospheric circulation conditions. In addition to examining trends over the entire period of record, we investigate trends

over the two halves separately as a simple way of characterizing their evolution. We note that the first half coincides with an upward trend in the NAM, while the second half coincides with a downward trend. We are particularly interested in assessing the evolving role of thermodynamic atmospheric circulation forcing of sea ice concentration trends, taking into account any seasonal dependencies. We use 5-day running mean sea ice concentration data on a 25 km  $\times$  25 km grid derived from passive microwave measurements from 1 January 1979 through 31 October 2007. Early results were presented by Deser and Teng [2008] for the winter and summer seasons only.

Our study is organized as follows. Section 2 describes the data sets and methodology. Section 3.1 provides results on trends in Arctic sea ice extent throughout the annual cycle, as well as derived quantities such as the timing of the seasonal cycle. Section 3.2 presents the spatial patterns of sea ice concentration, sea level pressure, and wind-induced atmospheric thermal advection trends for the two halves of the study period and for the record as a whole, stratified by season. Air temperature, sea surface temperature (SST), and net surface downward longwave radiation trends from 1979 to present are also shown. Section 4 provides a summary and discussion of the results.

## 2. DATA AND METHODS

Daily sea ice concentrations (SIC) on a 25 km  $\times$  25 km grid for the period 1 January 1979 to 31 October 2007 were obtained from the National Snow and Ice Data Center. These data are derived from the Nimbus 7 Scanning Multichannel Microwave Radiometer and Defense Meteorological Satellite Program (DMSP) F8, F11, and F13 Special Sensor Microwave/Imager radiances using the NASA team algorithm [Cavalieri et al., 1999].

In addition to daily SIC, we use monthly mean sea level pressure (SLP), 1000 hPa zonal and meridional wind components, 2-m and 1000-hPa air temperatures on a 2.5°  $\times$  2.5° latitude grid from the National Centers for Environmental Prediction/National Center for Atmospheric Research (NCEP/NCAR) reanalysis project [Kalnay et al., 1996] for the period January 1979 through October 2007. We also use monthly mean sea surface temperature data from the HadISST1 data set [Rayner et al., 2003] on a 1°  $\times$  1° latitude grid, updated through December 2006. The NCEP/NCAR reanalysis and HadISST1 data sets were obtained from the Data Support Section at NCAR. Finally, we make use of daily net surface downward longwave radiative fluxes derived from the NASA-NOAA Television and Infrared Observation Satellite (TIROS) Operational Vertical Sounder (TOVS) polar pathfinder data set [Francis and Hunter,

2007]. These data are available from July 1979 through December 2005 on a 100-km<sup>2</sup> grid north of 55°N.

### 3. RESULTS

#### 3.1. Arctic Sea Ice Extent

A map of the locations of the Arctic and sub-Arctic seas referred to in this study are shown in Figure 1. These place names are superimposed upon the long-term mean distributions of maximum and minimum sea ice extent (defined as marine areas within which sea ice concentrations equal or exceed 15%), based on the period 1979–2006. The maxi-

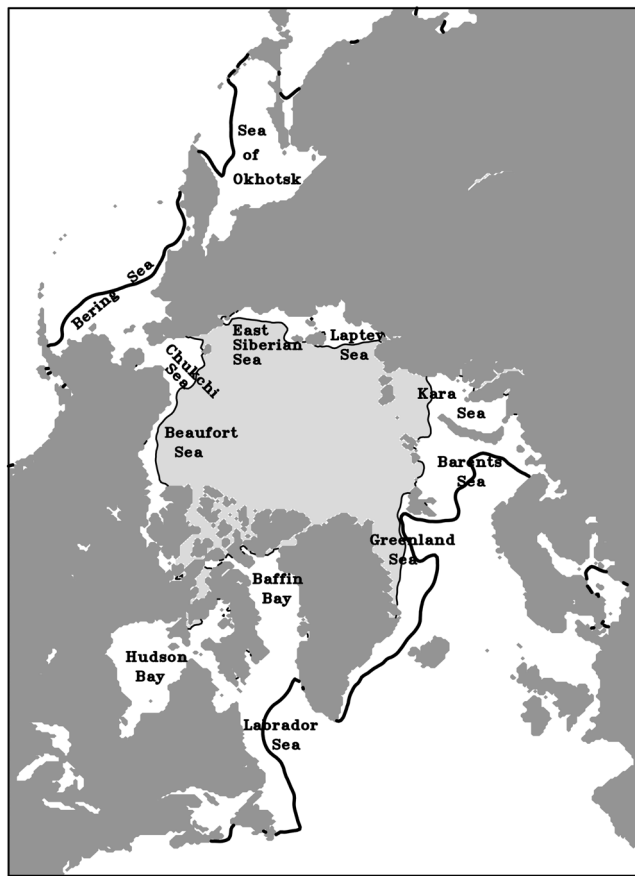


**Figure 1.** Locations of the Arctic and sub-Arctic seas referred to in this study, superimposed upon the long-term (1979–2007) mean sea ice extent at month of maximum (thick black contour) and month of minimum (thin black contour and light shaded areas). The maximum (minimum) sea ice extent is defined as the 30-day average centered on the mean date of maximum (minimum) extent, 7 March (17 September).

imum sea ice extent is defined as the 30-day average centered on the mean date of maximum extent, 7 March, and the minimum extent is defined as the 30-day average centered on the mean date of minimum extent, 17 September. At maximum extent, all of the Arctic and sub-Arctic seas are ice covered (sea ice concentrations >15%), while at minimum extent, only the Greenland and Beaufort seas and the Arctic basin (central Arctic Ocean) are ice covered.

Arctic sea ice extent serves as a useful starting point for describing the temporal character of sea ice over the Arctic as a whole. Following convention, we have defined Arctic sea ice extent as the area of the ocean covered by at least 15% sea ice concentration based on 5-day running mean data; note that Hudson Bay and the Baltic Sea have been excluded from this calculation. Plate 1 shows the 5-day running mean Arctic sea ice extent during the period 1 January 1979 to 31 October 2007, with each year overlaid in a different color (see color scale to the right of Plate 1). Plate 1 conveys the regularity of the seasonal cycle throughout the period of record, with maximum values ( $14\text{--}16 \times 10^6$  km<sup>2</sup>) occurring in early March and minimum values ( $5\text{--}7.5 \times 10^6$  km<sup>2</sup> excluding 2007) in the middle of September. In addition to the regularity of the seasonal cycle, Plate 1 conveys the systematic reduction of Arctic sea ice extent over time, with the 1980s exhibiting the highest values (red hues) and the 2000s showing the lowest values (blue hues). This systematic retreat of Arctic sea ice extent has occurred in all months of the year. Arctic sea ice extent reached unprecedented minimum values in August–October of 2007 (purple curve). The change in September sea ice extent between 2006 and 2007 alone ( $\sim 1.5 \times 10^6$  km<sup>2</sup>) is approximately equivalent to the entire change that occurred between September 1979 and September 2006 ( $\sim 1.3 \times 10^6$  km<sup>2</sup>).

The 5-day running mean Arctic sea ice extent data shown in Plate 1 are replotted in Figure 2 (top) as a single continuous time series starting on 1 January 1979 and ending on 31 October 2007. The same record after removing the long-term 5-day running mean seasonal cycle is shown in Figure 2 (bottom). The former depiction serves to emphasize that the seasonal cycle of Arctic sea ice extent is still the most prominent feature of the record, while the latter underscores the accelerating downward trend of Arctic sea ice extent over time. Arctic sea ice extent has declined at a rate of  $-0.52 \times 10^6$  km<sup>2</sup> per decade, or  $-1.76 \times 10^6$  km<sup>2</sup> over the period 1 January 1979 to 1 January 2007; this trend is significant at the 99% level. The magnitude of the downward linear trend has increased from  $-0.35 \times 10^6$  km<sup>2</sup> per decade to  $-0.9 \times 10^6$  km<sup>2</sup> per decade from the first half (January 1979 to December 1993) to the second half (January 1993 to October 2007) of the record (similar results were found by Comiso *et al.* [2008]).

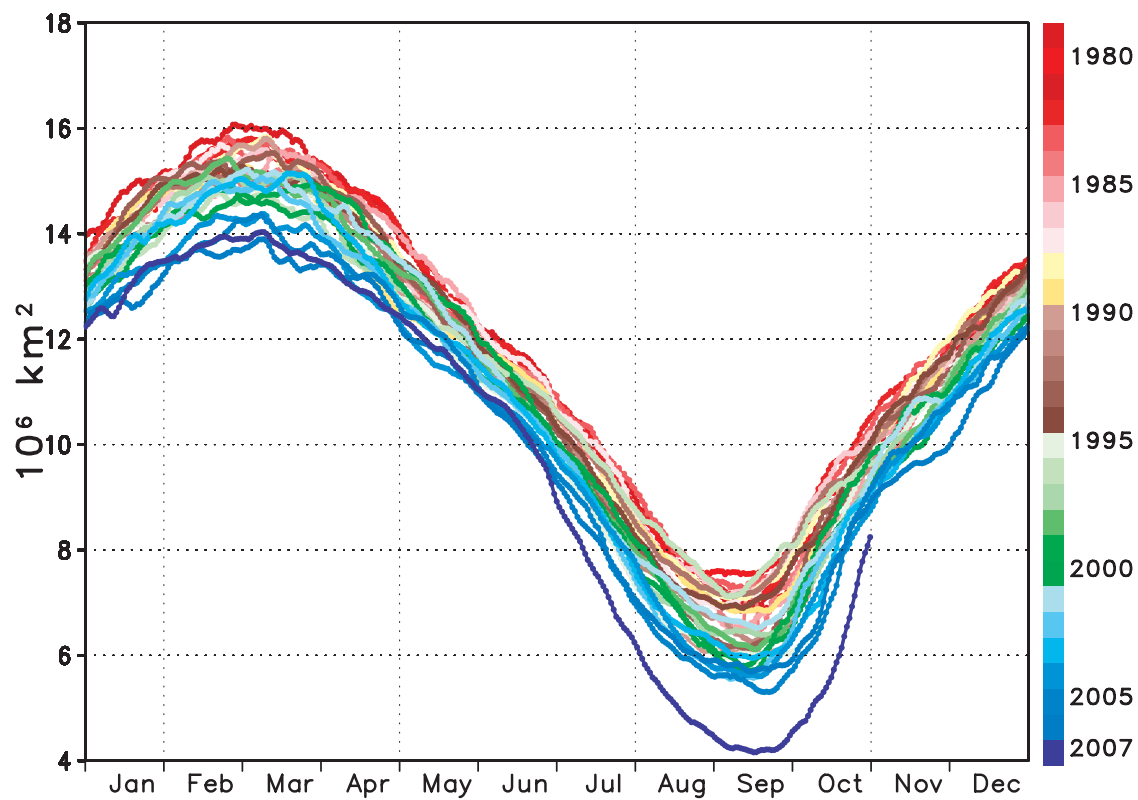


**Plate 1.** Five-day running mean Arctic sea ice extent ( $10^6 \text{ km}^2$ ) during the period 1 January 1979 to 31 October 2007, with each year overlaid in a different color (see color scale at right). Arctic sea ice extent is defined as the area of the ocean covered by at least 15% sea ice concentration.

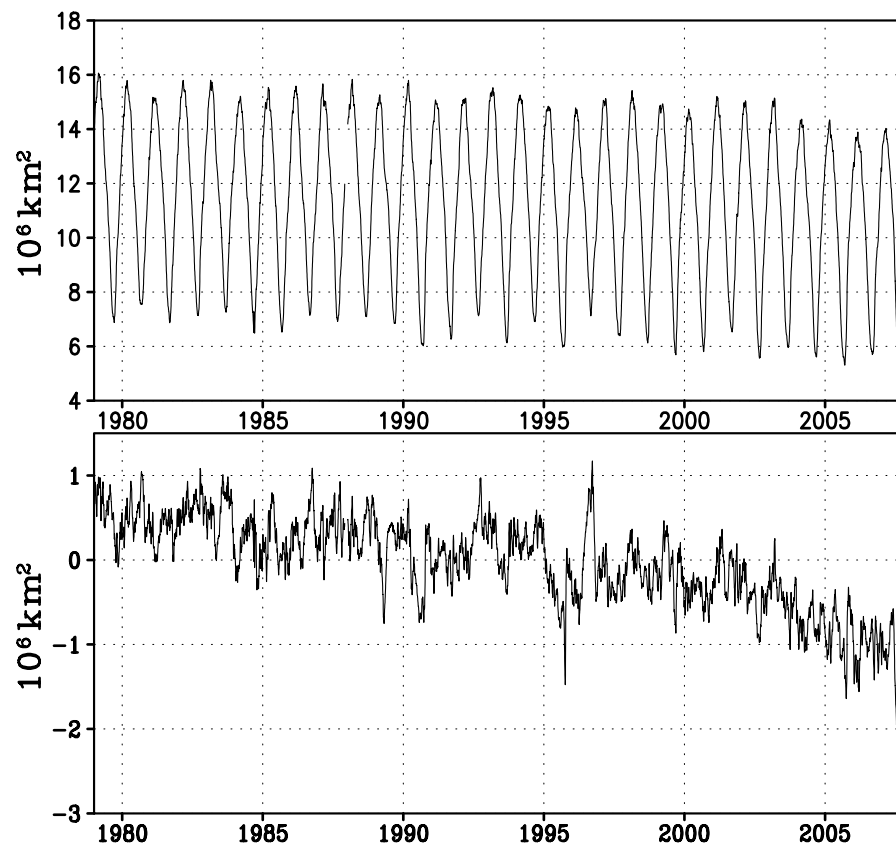


**Figure 2.** Time series of 5-day running mean Arctic sea ice extent ( $10^6 \text{ km}^2$ ) from 1 January 1979 to 31 October 2007 (top) with and (bottom) without the long-term mean seasonal cycle.

Figure 3 isolates the behavior of the maximum and minimum values of sea ice extent shown in Plate 1 and their dates of occurrence during 1979–2007. Minimum and maximum values were determined by comparing adjacent 5-day running means. Linear trend lines in the dates and values of maximum and minimum Arctic sea ice extent, determined by linear least squares “best fit” regression lines to the 5-day running mean data during January 1979 to June 2007 (note that data after June 2007 were purposefully omitted from this calculation), are superimposed on the original time series in Figure 3. Figure 3 (left) shows that there has been a downward trend in both the maximum and minimum sea ice extent values ( $-0.5 \times 10^6 \text{ km}^2$  per decade and  $-0.7 \times 10^6 \text{ km}^2$  per decade, respectively; significant at the 99% level), with a corresponding increase in the amplitude of the annual cycle ( $0.15 \times 10^6 \text{ km}^2$  per decade, although this does not pass the 90% significance threshold). In terms of percentage of the mean maximum ( $15.2 \times 10^6 \text{ km}^2$ ) and mean minimum ( $6.4 \times 10^6 \text{ km}^2$ ) sea ice extent, the downward trends in maximum and minimum extent are  $-9.0\%$  per decade and  $-3.4\%$  per decade, respectively.

The time series of the dates of maximum and minimum sea ice extent (Figure 3, right) show that there has been a slight upward trend (indicative of a progressively later date) in the date of maximum sea ice extent of 4 days per decade (or 12 days over the period 1979–2007; significant at the 90% level), while there has been little change in the date of minimum ice extent (1 day per decade). The length of time between maximum and minimum extent has decreased slightly at a rate of 3 days per decade or 9 days over the period January 1979 to June 2007, but this does not pass the 90% significance threshold. The mean dates of maximum and minimum sea ice extent occur on 7 March and 17 September, respectively. It should be noted that the record low minimum sea ice extent in 2007 occurred on 16 September, close to the mean date of minimum sea ice extent.

The magnitude and sign of the linear trends in Arctic sea ice extent as a function of time of year are shown in Figure 4 based on 5-day running mean data for the period 1 January 1979 to 30 June 2007 (the record low values since June 2007 are purposefully omitted from the trend calculation). The trends are expressed in terms of actual magnitude (square

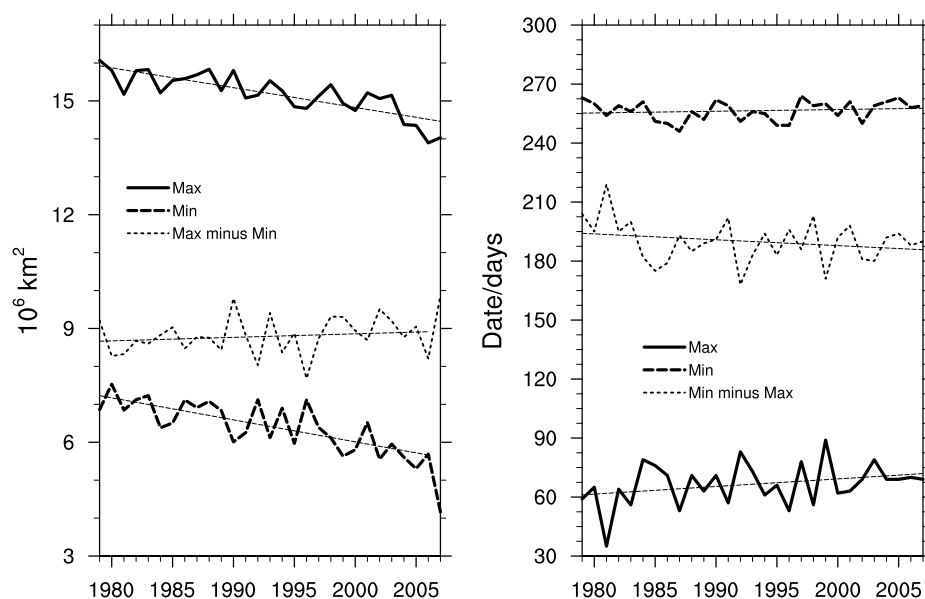


**Figure 3.** Time series of maximum (solid curves) and minimum (long dashed curves) values of (left) Arctic sea ice extent ( $10^6 \text{ km}^2$ ) and (right) their dates of occurrence, determined from 5-day running mean data. The dotted curves show the time series of the maximum-minus-minimum sea ice extent and the date of minimum extent minus the date of maximum extent. Linear trend lines are superimposed using data before 1 June 2007.

kilometers per decade) and relative magnitude (percent per decade, taken with respect to the long-term mean extent for each 5-day running mean period). All trend values are statistically significant at the 95% level. The linear trend is negative at all times of year, with the largest magnitudes ( $0.55$  to  $0.65 \times 10^6 \text{ km}^2$  per decade or 7 to 10% per decade) from the end of July to the middle of October when the mean sea ice extent is smallest (recall Plate 1). The relative magnitude of the trend has a larger seasonal dependence than the actual magnitude, ranging from a maximum value of nearly  $-10\%$  per decade in mid September to a minimum value of  $-3$  to  $-4\%$  per decade from November through June. The actual magnitude of the trend ranges from a maximum value of  $-0.65 \times 10^6 \text{ km}^2$  per decade in early October to a minimum value of  $-0.4$  to  $-0.5 \times 10^6 \text{ km}^2$  per decade from November through June.

Trends in the dates of maximum and minimum sea ice extent were presented in Figure 3 (right). Another approach to characterizing the timing of the seasonal cycle is to examine the date when sea ice concentration first falls below 50% and when it first exceeds 50% at each grid point for each year. Plate 2 shows the geographical distributions of the trends in these dates along with the corresponding long-term mean

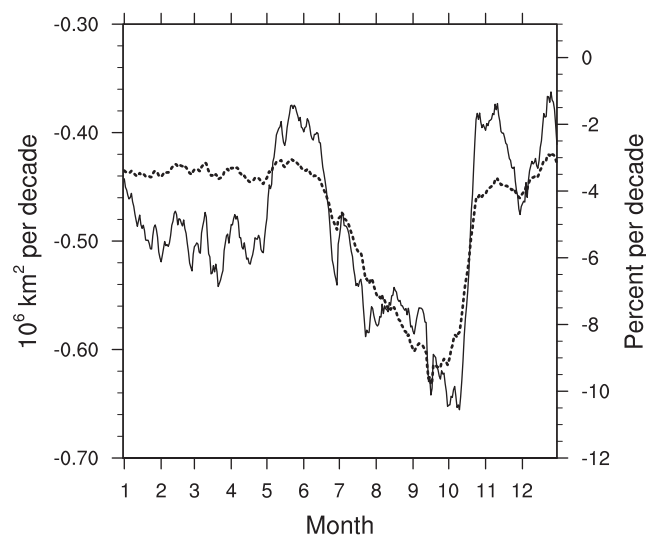


**Figure 4.** Linear trends in Arctic sea ice extent as a function of time of year based on 5-day running mean data for the period 1 January 1979 to 30 June 2007, expressed in terms of actual magnitude ( $\text{km}^2$  per decade, solid curve) and relative magnitude (percent per decade, taken with respect to the long-term mean extent for each 5-day running mean period, dotted curve).

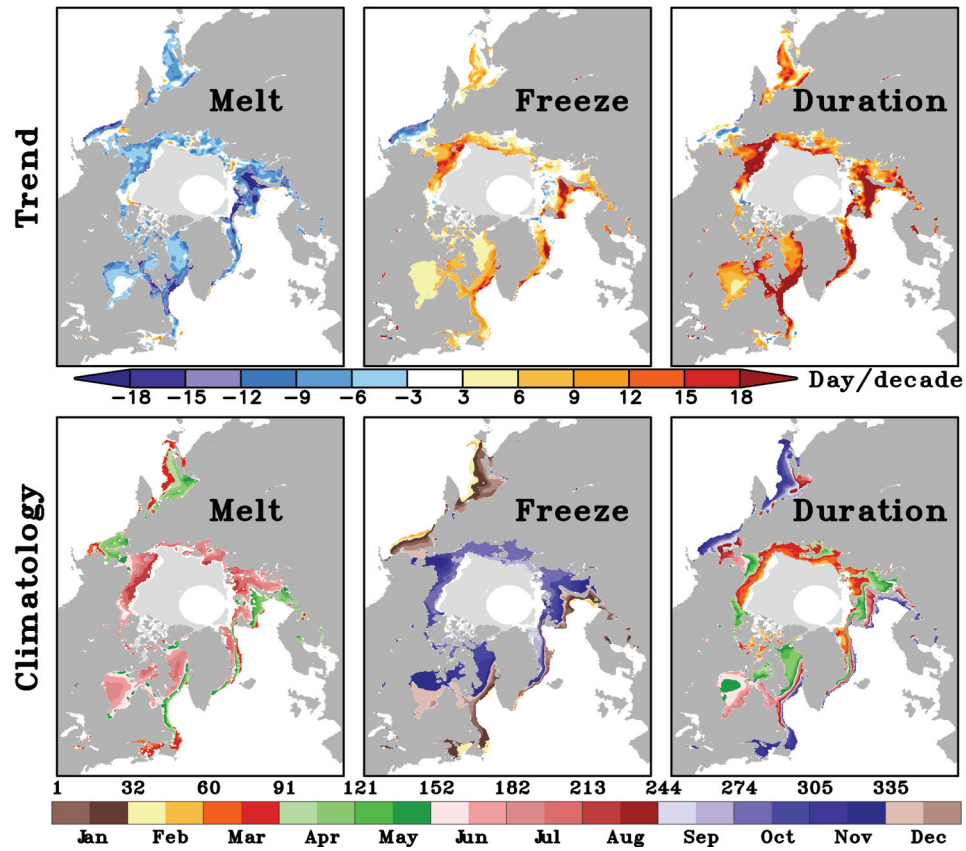


**Plate 2.** Geographical distributions of the (top) linear trends and (bottom) climatologies of the dates when sea ice concentration first falls below 50% (“melt”), first exceeds 50% (“freeze”), and their difference (“duration”) based on 5-day running mean data during 1979–2006. The trend values are expressed in days per decade, and the climatological values are expressed in terms of calendar date (number of days for “duration”). The white ellipse around the North Pole indicates missing data.

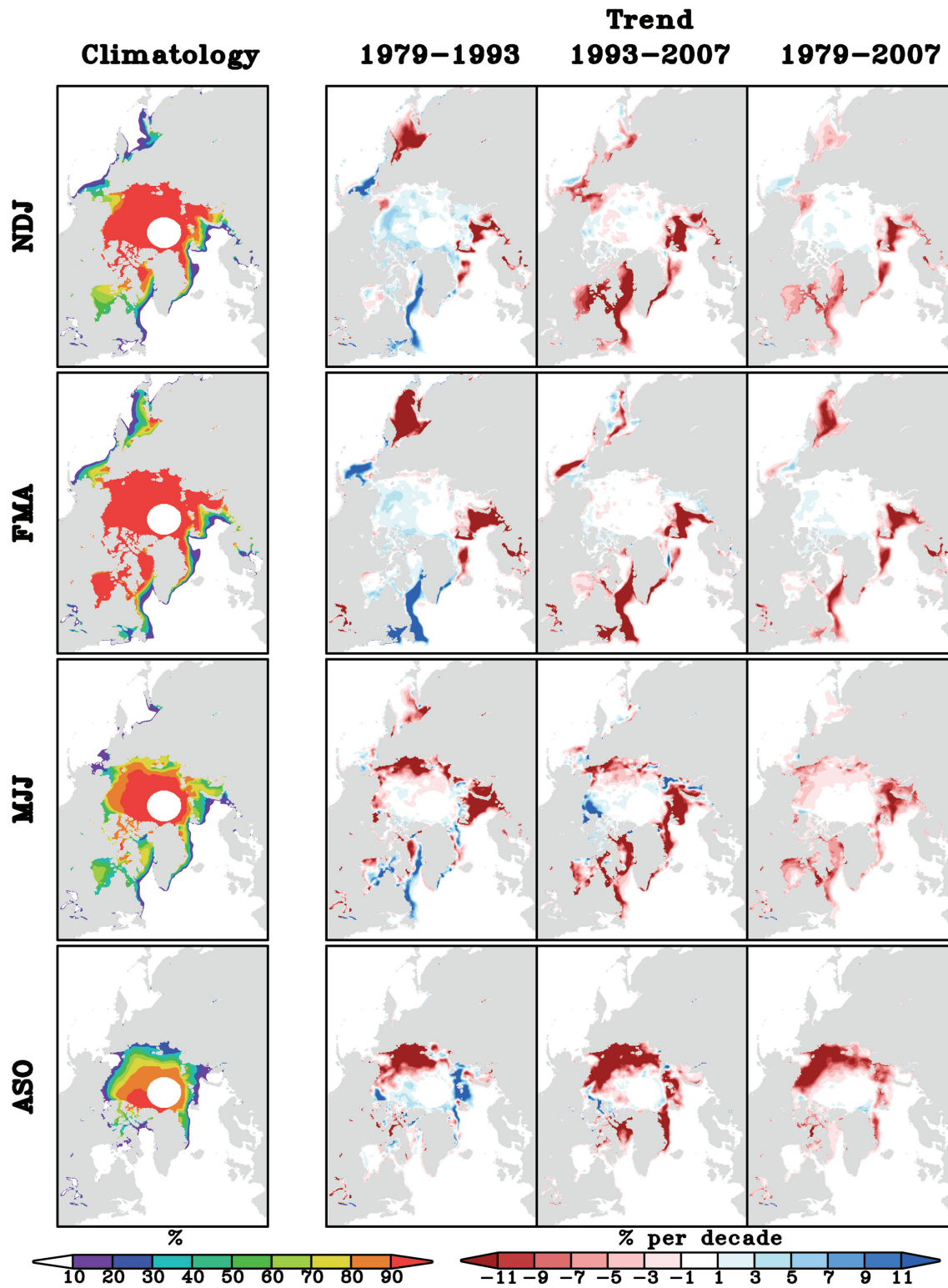


**Plate 3.** Seasonal mean sea ice concentration (far left panels) climatologies based on the period 1979–2007 (percent) and linear trends (percent per decade) during (left) 1979–1993, (middle) 1993–2007, and (right) 1979–2007. Data after 30 April 2006 are excluded. Seasons are defined as (first row) November–January (NDJ), (second row) February–April (FMA), (third row) May–July (MJJ), and (fourth row) August–October (ASO). The white ellipse around the North Pole indicates missing data.

values, based on 5-day running means during January 1979 to June 2007. The linear trends in the dates when SIC first falls below 50% are consistently negative throughout the Arctic, with amplitudes  $\sim 6$ –9 days per decade in many regions and even greater values in the Barents Sea (Plate 2, top left). Similarly, the linear trends in the dates when SIC first exceeds 50% are positive throughout the marginal ice zone except in the Bering Sea, with amplitudes  $\sim 6$ –12 days per decade (12–18 days per decade in the Barents and Chuckchi seas; Plate 2, top middle). These patterns result in large positive trends in the duration of SIC  $< 50\%$ , with values in excess of 18 days per decade in the Labrador, Greenland, Barents and Chuckchi seas (Plate 2, top right). The spatial uniformity of the trend values in all three quantities (Plate 2, top panels) contrasts with the large meridional gradients present in their background climatologies (Plate 2, bottom). Qualitatively similar results are obtained with thresholds of 30% and 70% (not shown).

Figure 5 shows the time series of the area-averaged dates when SIC first falls below or exceeds 50%. There is a trend toward an earlier (later) date of occurrence of sea ice concentrations first falling below (exceeding) 50% of  $-3.0$  days per decade (3.7 days per decade). This results in an increasing trend in the duration of SIC  $< 50\%$  (defined as the difference between the dates when SIC first falls below 50% and first exceeds 50%) of 6.9 days per decade or 19 days over the period

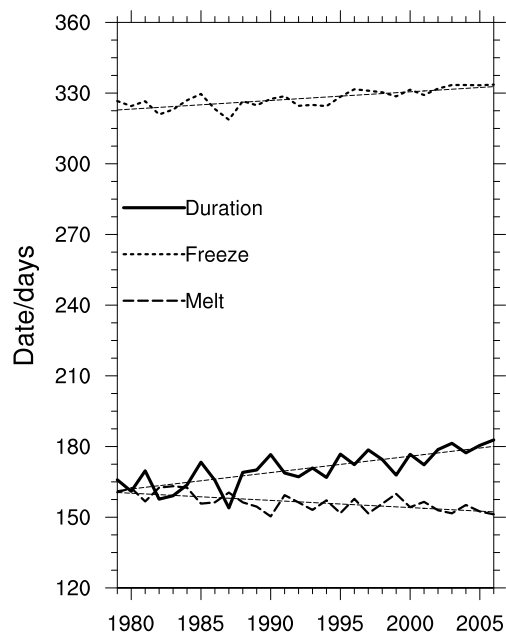


**Figure 5.** Time series of the area-averaged dates when SIC first falls below 50% (“melt,” dashed curve), first exceeds 50% (“freeze,” dotted curve), and their difference (“duration,” solid curve).

1979–2006, statistically significant at the 99% level. The duration of the sea ice melt season, determined from emissivity changes associated with liquid and frozen water, has shown an even larger increase (approximately 2 weeks per decade [Stroeve *et al.*, 2006]) than the duration of SIC  $< 50\%$ .

### 3.2. Arctic Sea Ice Concentration

**3.2.1. SIC trends.** Up to now, we have focused on trends in sea ice extent for the Arctic as a whole. In this section, we consider the spatial patterns of recent trends in Arctic sea ice concentration (SIC), taking into account the seasonal dependence of the trends. To reduce the amount of information, we focus on 3-month seasons defined as follows: November–January (NDJ); February–April (FMA); May–July (MJJ); and August–October (ASO); we refer to these seasons as autumn, winter, spring, and summer, respectively. This choice of seasonal averaging retains the basic characteristics of the annual cycle and seasonal dependence of recent trends. The spatial patterns of the monthly SIC trends are highly coherent within each season (not shown).

The climatological SIC distributions for each season based on the period January 1979 to April 2007 are shown in the far left-hand column of Plate 3. In winter (FMA), the season of maximum sea ice extent, long-term mean SIC values between 10% and 90%, indicative of the location of the marginal ice zone, are found in the Labrador Sea, the Greenland and Barents seas, the Bering Sea, and the Sea of Okhotsk. In summer (ASO), the season of minimum sea ice extent, the marginal ice zone retreats northward to coastal regions of the Arctic Ocean and the Canadian Archipelago. The long-term mean SIC distribution in autumn (NDJ) resembles that in winter, albeit with reduced values in the peripheral seas, particularly the Bering Sea and the Sea of Okhotsk. The climatological SIC distribution in spring (MJJ) is not identical to that in autumn: although similar values prevail over the Atlantic sector, lower amounts occur within coastal regions of the central Arctic Ocean, and the Pacific marginal seas are nearly ice free.

These climatological SIC distributions provide a context for the spatial patterns of recent SIC trends shown in the left, middle, and right columns of Plate 3. In addition to showing the trends over the full period of record (January 1979 to June 2007), Plate 3 also shows the evolution of the trends from the first half of the record (January 1979 to December 1993) to the second (January 1993 to June 2007). Note that the magnitudes of the trends in each period may be directly compared as they are expressed in percent SIC per decade. The regions of largest-amplitude SIC trends in each season correspond to the marginal ice zone as depicted in the left-hand columns. As a general rule of thumb, SIC trends exceeding 3% per decade in absolute value (corresponding to

the second level of red or blue shading in Plate 3) are statistically significant at the 95% level.

The pattern of winter SIC trends in the first half of the record (1979–1993) exhibits positive values in the Labrador and Bering seas and negative values in the Greenland and Barents seas and the Sea of Okhotsk. In contrast, winter SIC trends in the second half of the record (1993–2007) are negative throughout the marginal seas, with the largest declines in the Atlantic sector. The winter SIC trends over the full period of record (1979–2007) are also negative throughout the marginal seas, except in the Bering Sea where the trends are near zero. The change in pattern of winter SIC trends between the first and second halves of the record is notable and will be discussed further below in the context of evolving atmospheric circulation trends. The patterns of SIC trends in the autumn season are very similar to those in winter, with somewhat reduced magnitudes commensurate with the lower long-term mean SIC amounts.

In summer, SIC trends in the first half of the record are negative in the East Siberian Sea and positive in the Barents, Kara, and eastern Beaufort seas, with the area of reduced SIC outweighing that of increased SIC. In the second half of the record (1993–2006), the area of negative SIC trends has expanded to cover almost all longitudes. The summer SIC trend over the full period of record (1979–2006) is similar to that for the second half of the record, with the largest declines extending from the Laptev Sea eastward to the Beau-

fort Sea. The SIC trends in spring are a mixture of those in winter and summer. In particular, the trends in the Atlantic sector follow those in winter, while the trends in the central Arctic Ocean resemble those in summer but with weaker magnitudes. The hybrid nature of the spring SIC trends is consistent with that of the long-term mean SIC distribution discussed earlier.

It is instructive to relate the results shown in Plate 3 back to the behavior of sea ice extent for the Arctic as a whole. Figure 6 shows the linear trends in Arctic sea ice extent as a function of time of year based on 5-day running means for the two halves of the record separately (excluding data since June 2007). Trend values significant at the 95% level are shown with a bold line segment. Note that the magnitudes of the trends in each period may be directly compared as they are expressed in square kilometers per decade and percent of the period mean per decade. The negative trends in Arctic sea ice extent increased dramatically in magnitude between the first and second halves of the record during October–March, from values of 0 to  $-0.3 \times 10^6 \text{ km}^2$  (0 to  $-2\%$ ) per decade to values of  $-0.8$  to  $-1.1 \times 10^6 \text{ km}^2$  ( $-6$  to  $-8\%$ ) per decade. The weak and statistically insignificant trends in the first half of the record are due to the large degree of cancellation between negative and positive SIC trends in different regions not to a lack of SIC trends (recall Plate 3). In terms of actual magnitude (Figure 6, left), the seasonal dependence of the trend amplitudes is nearly opposite between the two

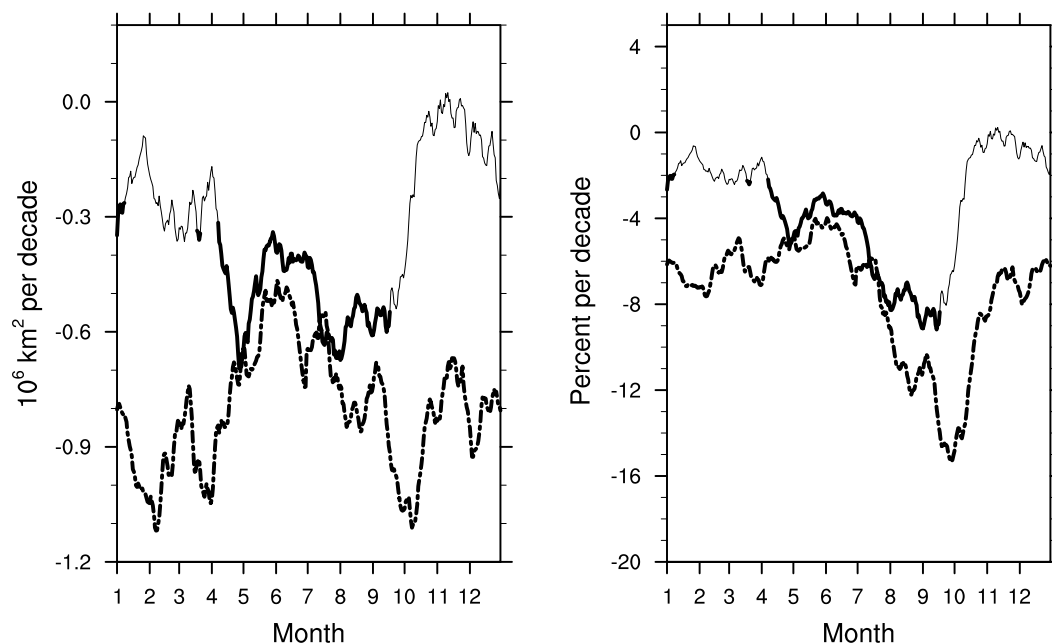


**Figure 6.** As in Figure 4 but for the first (1979–1993, solid curve) and second (1993–2007, dashed curve) halves of the record. Trend values significant at the 95% level are shown with a bold line segment.

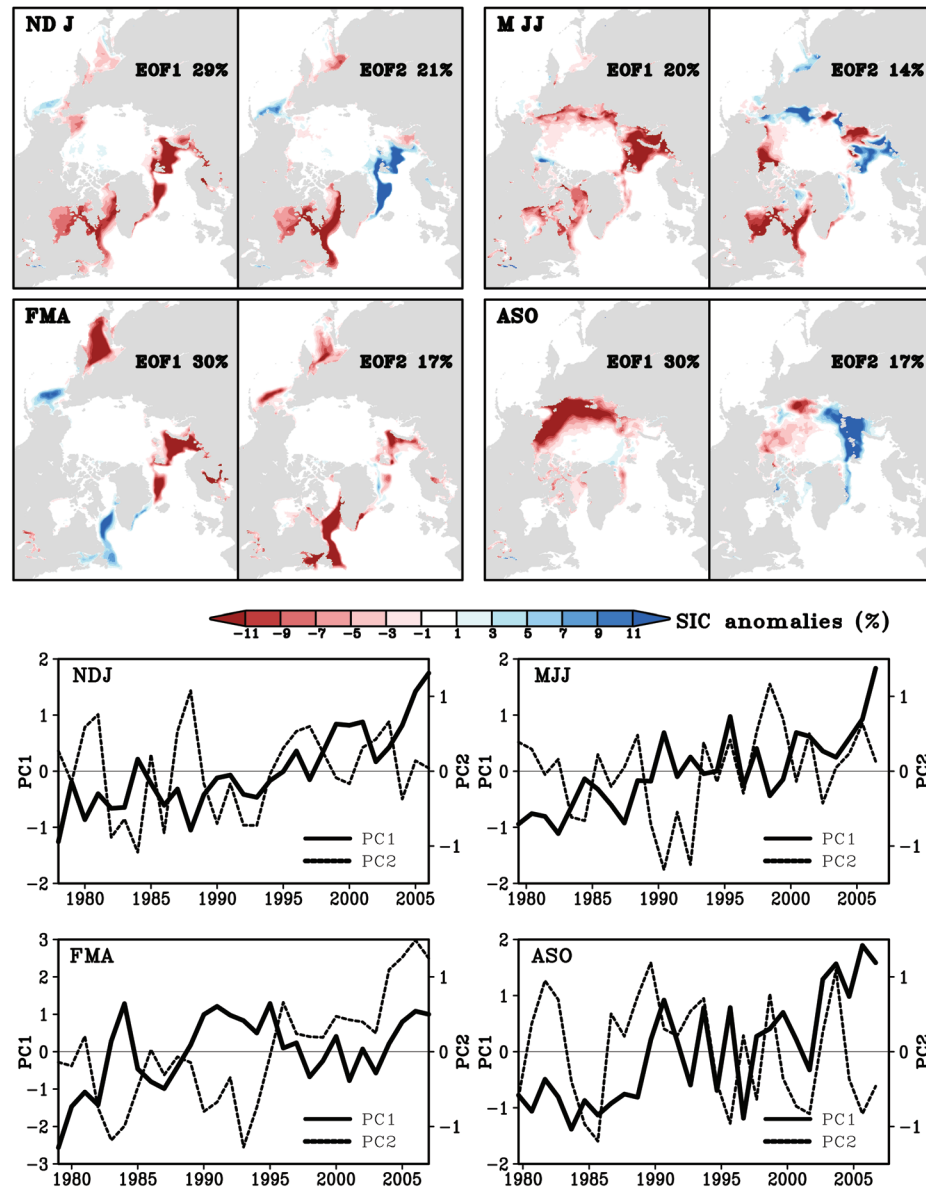


**Plate 4.** (top) EOFs 1 and 2 and (bottom) their associated principal component time series for each season based on the period January 1979 to April 2007. The percent variances explained are given in the EOF plots.

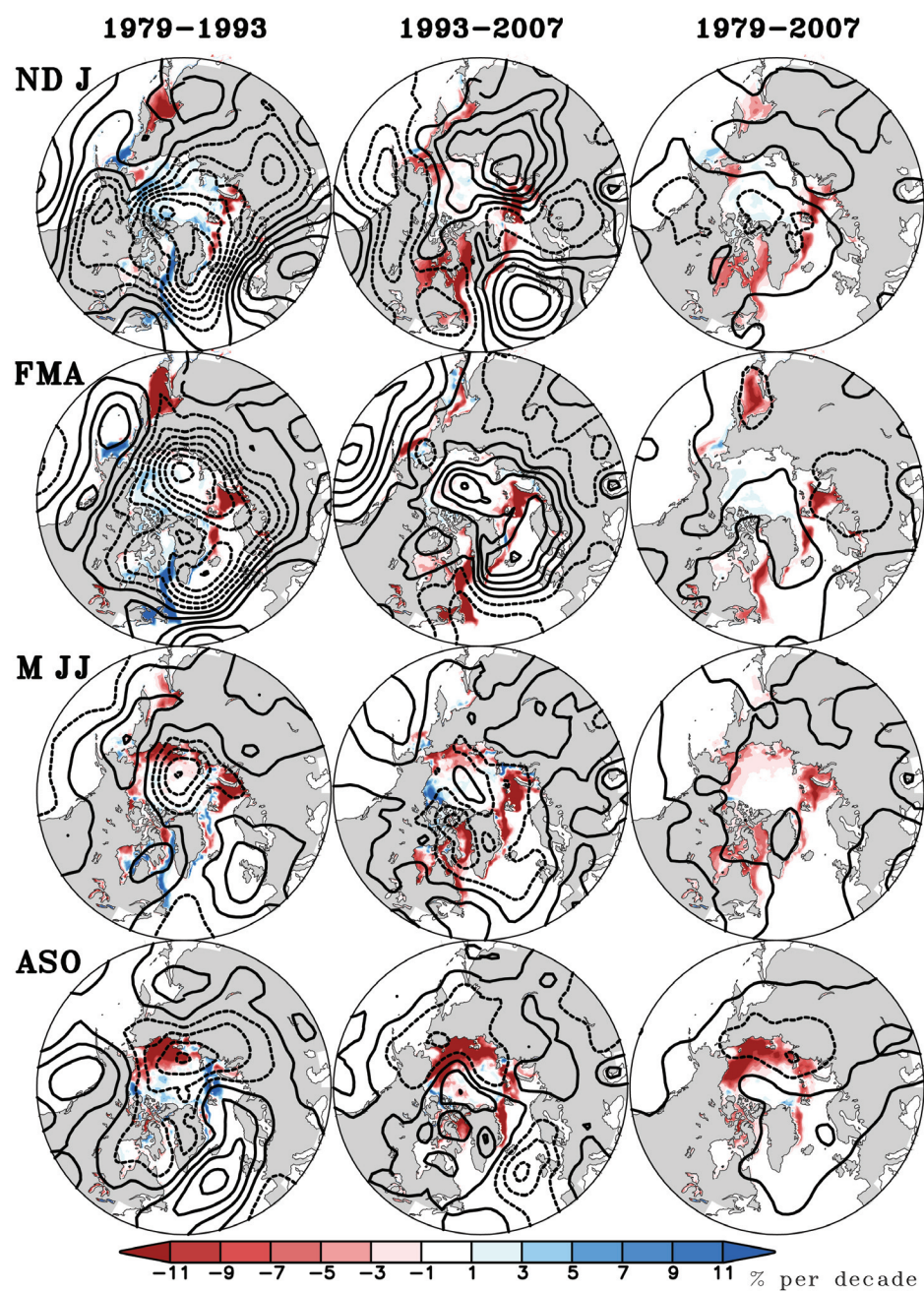


**Plate 5.** Sea ice concentration (color shading, percent per decade) and sea level pressure (contours, hPa per decade) trends during (left) 1979–1993, (middle) 1993–2007, and (right) 1979–2007 for each season as indicated. The contour interval for sea level pressure is 1 hPa per decade; negative values are dashed, and the zero and positive values are solid. Note that data after April 2007 are excluded.

halves of the record, with the smallest (largest) trends occurring during the cold season (October–March) during the first (second) half of the record. In terms of relative magnitude (Figure 6, right), the seasonality of the trends in Arctic sea ice extent remains similar between the two periods, with the largest negative trends occurring during summer (mid July to early October). The maximum relative trend amplitudes have shifted from mid September in the first half of the record to late September in the second half, and they have also amplified (9% per decade in the first half to 15% per decade in the second half).

*3.2.2. Empirical orthogonal function analysis of SIC anomalies.* Are the SIC trend patterns shown in Plate 3 preferred structures of variability, or are they simply a result of dividing the record into halves? To address this question, we have applied empirical orthogonal function (EOF) analysis to seasonal SIC anomaly fields over the full period of record, using a separate EOF analysis for each season. Note that the SIC anomalies have not been normalized by their standard deviation for this calculation. The two leading EOFs in each season and their associated principal component (PC) time series are shown in Plate 4. In both winter and summer, the first and second EOFs account for 30% and 17% of the variance, respectively. In autumn (spring), EOF1 accounts for 29% (20%) of the variance and EOF2 for 21% (14%) of the variance. In all seasons, EOFs 1 and 2 are well separated according to the criterion of *North et al.* [1982].

In winter, the leading EOF exhibits out-of-phase variations between the eastern and western Atlantic and between the eastern and western Pacific, strongly reminiscent of the trend pattern during the first half of the record (recall Plate 3). This EOF is nearly identical to that given by *Ukita et al.* [2007] based on February–March averages over the period 1979–2003 and consistent with results obtained using data sets beginning in the early 1950s [*Walsh and Johnson*, 1979; *Fang and Wallace*, 1994; *Deser et al.*, 2000]. The associated PC time series exhibits an upward trend from 1979 to 1995, near zero values from 1996 through 2004, and positive values from 2005 through 2007. EOF2 of winter SIC is characterized by uniform polarity throughout the Arctic marginal ice zones, with largest amplitudes in the Labrador Sea. This EOF resembles the trend pattern during the second half of the record (recall Plate 3). Its PC time series exhibits generally negative values before 1995 and positive values thereafter, indicative of a decreasing trend of winter SIC in the peripheral seas. It is notable that the first and second EOFs of winter SIC anomalies during 1979–2007 correspond to the winter SIC trend patterns in the first and second halves of the record, respectively, indicating that these two trend patterns dominate the variability over the period of study. To

our knowledge, the only other study documenting the spatial pattern associated with EOF2 of winter SIC variability is that of *Deser and Teng* [2008].

The leading EOF of summer SIC anomalies during 1979–2006 exhibits uniform polarity throughout most of the Arctic marginal ice zone, with largest amplitudes from the Laptev Sea eastward to the Beaufort Sea (Plate 4). This EOF resembles closely the patterns of summer SIC trends during 1979–2006 and 1993–2006 and projects substantially onto the trend pattern for 1979–1993 (recall Plate 3). This similarity is consistent with the fact that the leading PC time series exhibits an upward trend over the period of record. The second EOF of summer SIC anomalies consists of out-of-phase variations between the Barents/Kara seas and the East Siberian/Beaufort seas, with no discernible trend in its PC time series. This EOF does not correspond closely to any of the summer SIC trend patterns shown in Plate 3, although it captures some of the out-of-phase behavior evident in the early period.

Although the SIC trend patterns in autumn resemble those in winter (especially over the Atlantic sector), the ordering of the EOFs is reversed, with the leading (second) EOF in winter corresponding to the second (leading) EOF in autumn (Plate 4). The leading EOF in spring consists of negative values throughout the marginal ice zone, similar to the trend patterns during 1993–2006 and 1979–2006, while the second EOF resembles the trend pattern during 1979–1993. Thus, the leading EOF of SIC anomalies in spring, summer, and autumn (and the second EOF in winter) exhibit negative values throughout the marginal ice zone, similar to the trend patterns since 1993 (and 1979). We expect that if the current winter SIC declines continue, the leading EOF for that season will also eventually exhibit negative values throughout the peripheral seas.

*3.2.3. SIC trends in the context of atmospheric circulation trends.* As discussed in section 1, our motivation for examining the two halves of the record separately is not only to assess in a simple fashion the evolution of the SIC trends over time but also to examine the SIC trends in the context of a rising and falling NAM index. Recall that the NAM is the leading pattern of atmospheric circulation variability over the extratropical Northern Hemisphere in all seasons [*Portis et al.*, 2001], and in winter it exhibits a positive trend in the first half of the record and a negative trend in the second half. To aid our interpretation of the role of SLP forcing of SIC trends, we also consider trends in wind-induced atmospheric thermal advection due to trends in the 1000 hPa zonal and meridional wind components advecting the time-mean zonal and meridional 1000 hPa air temperature gradients, respectively, for each time period considered.

Plate 5 shows the SIC trends in the context of overlying trends in SLP for the first half (1979–1993), second half (1993–2007), and full period of record (1979–2007); note the larger domain compared to Plate 3. We have omitted data after 30 April 2007 from the trend calculations to avoid biasing the results because of the unusually large sea ice extent reductions in summer 2007 (recall Plate 1). The SLP trends are based on the same seasonal definitions used for SIC and are very similar to those leading by 1 month (e.g., October–December; January–March; April–June; July and September are not shown). The simultaneous (or 1-month lead) relationships between seasonal SLP and SIC trends provide an indication of the role of atmospheric circulation forcing of sea ice anomalies [see, e.g., Fang and Wallace, 1994]. However, there may also be a longer response time (e.g., seasonal and multiyear) associated with atmospheric forcing of sea ice thickness changes, which, in turn, feedback upon SIC [Rigor et al., 2002; Rigor and Wallace, 2004; Nghiem et al., 2007]. This component of the SIC response to atmospheric circulation forcing will not be addressed with our approach. The accompanying seasonal trends in 1000-hPa atmospheric thermal advection as defined above are shown in Plate 6.

We consider first the trends in autumn and winter. In these two seasons, SLP trends in the first half of the record resemble the positive phase of the NAM, with negative values over the Arctic and northern North Atlantic (maximum amplitudes  $\sim 4\text{--}6$  hPa per decade) and positive values farther south (Plate 5). This pattern results in anomalous northwesterly winds over the enhanced sea ice cover in the Labrador and Bering seas and anomalous southerly winds over the regions of reduced ice cover in the Greenland and Barents seas and the Sea of Okhotsk. These wind anomalies advect cold air over the Labrador and Bering seas and warm air over the Greenland and Barents seas and the Sea of Okhotsk and thus contribute thermodynamically to forcing the pattern of SIC trends (Plate 6).

The pattern of winter SLP trends in the second half of the record is largely opposite to that in the first half over the Arctic and north Atlantic sectors, consistent with the behavior of the winter NAM index which reached a relative maximum in the early 1990s (the winter SLP trends over the north Pacific do not reverse sign between the two halves of the record). The inferred geostrophic wind trends are indicative of enhanced southeasterly (southwesterly) flow, which, in turn, results in anomalous warm advection, over the reduced SIC in the Labrador Sea (Bering Sea, Plate 6). Thus, the change in sign of the winter SIC trends in the Labrador and Bering seas between the two halves of the record may be attributed at least in part to the change in sign of the overlying wind and associated thermal advection trends. The persistence of negative winter SIC trends in the Barents seas in the second half of the

record is also consistent with the continued trend of enhanced warm air advection because of low-level wind changes.

Spring and summer SLP trends in the first half of the record exhibit a low-pressure center over the Arctic Ocean, a pattern which results in southerly geostrophic wind anomalies over the negative spring and summer SIC trends in the East Siberian, Chukchi and Beaufort seas (Plate 5). These wind anomalies, in turn, drive increased warm air advection, consistent with the notion that atmospheric circulation changes contribute to the SIC anomalies in these regions (Plate 6). The northerly wind trends that occur over the positive SIC trends in the Barents and Kara seas in summer in the first half of the record are also indicative of the role of atmospheric circulation forcing via enhanced cold air advection. However, the negative SIC trends in spring in these regions do not appear to be forced by wind-induced atmospheric thermal advection.

In the second half of the record, spring and summer SLP trends over the Arctic are relatively weak, as are the accompanying trends in low-level thermal advection (Plates 5 and 6). Thus, the large sea ice losses in the second half of the record in spring and summer do not appear to be due to trends in atmospheric thermal advection.

Over the record as a whole (1979–2007), SLP trends in all seasons are weak, with magnitudes generally less than 1 hPa per decade (Plate 5). The accompanying trends in wind-induced atmospheric thermal advection are also generally weak (the Barents Sea in fall is an exception) and even negative in many areas of the marginal ice zone (Plate 6).

As discussed in section 1, other factors besides atmospheric circulation forcing are contributing to the long-term Arctic sea ice loss, including higher air temperatures [Comiso, 2003; Serreze et al., 2007; Comiso et al., 2008], increased net downward longwave radiation [Francis and Hunter, 2006, 2007], warmer SSTs [Polyakov et al., 2005; Steele et al., 2008], positive ice-albedo feedback [Perovich et al., 2007], and thinning of the ice pack [Lindsay and Zhang, 2005; Nghiem et al., 2007]. Plate 7 confirms that the trends in near-surface (2 m) air temperatures, SSTs, and net downward longwave radiation during 1979–2007 are positive (and statistically significant at the 95% confidence level) over much of the Arctic and adjacent seas in each season. Air temperatures have risen by more than  $1^\circ\text{C}$  per decade in summer, fall, and winter and by up to  $0.7^\circ\text{C}$  per decade in spring. SSTs have warmed significantly in the North Atlantic, Pacific, and sub-Arctic seas, with the largest increases (up to  $0.9^\circ\text{C}$  per decade) in summer in the Labrador, East Siberian, and Chukchi seas. Net surface downward longwave radiation has also increased at high latitudes, with significant trends in all seasons except winter and the largest trends in summer (maximum values of  $12\text{--}20$   $\text{W m}^{-2}$  per decade). Collectively,

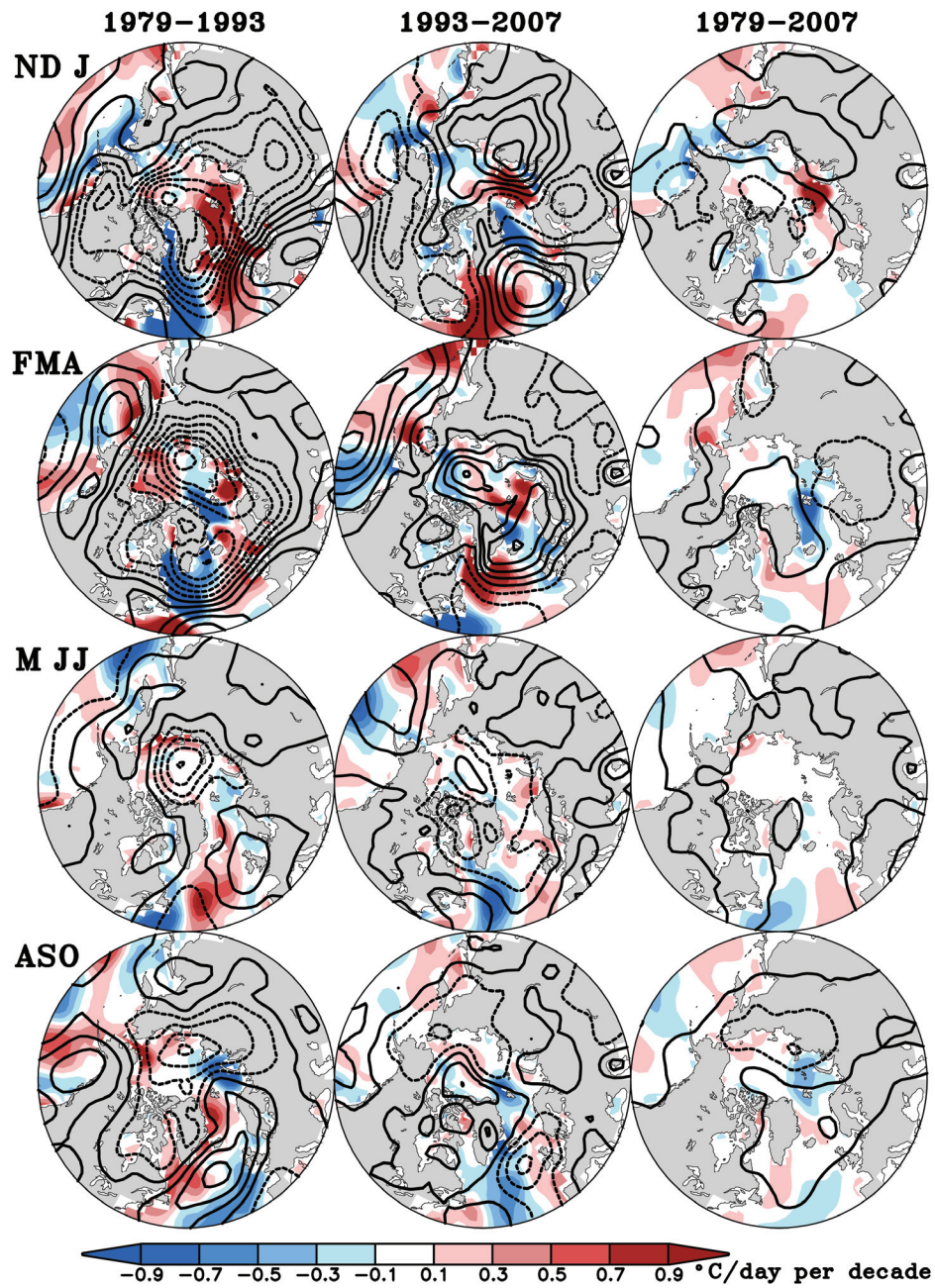


**Plate 6.** As in Plate 5 but for wind-induced 1000-hPa atmospheric thermal advection ( $^{\circ}\text{C}/\text{d}$  per decade). Thermal advection trends over land are not shown.

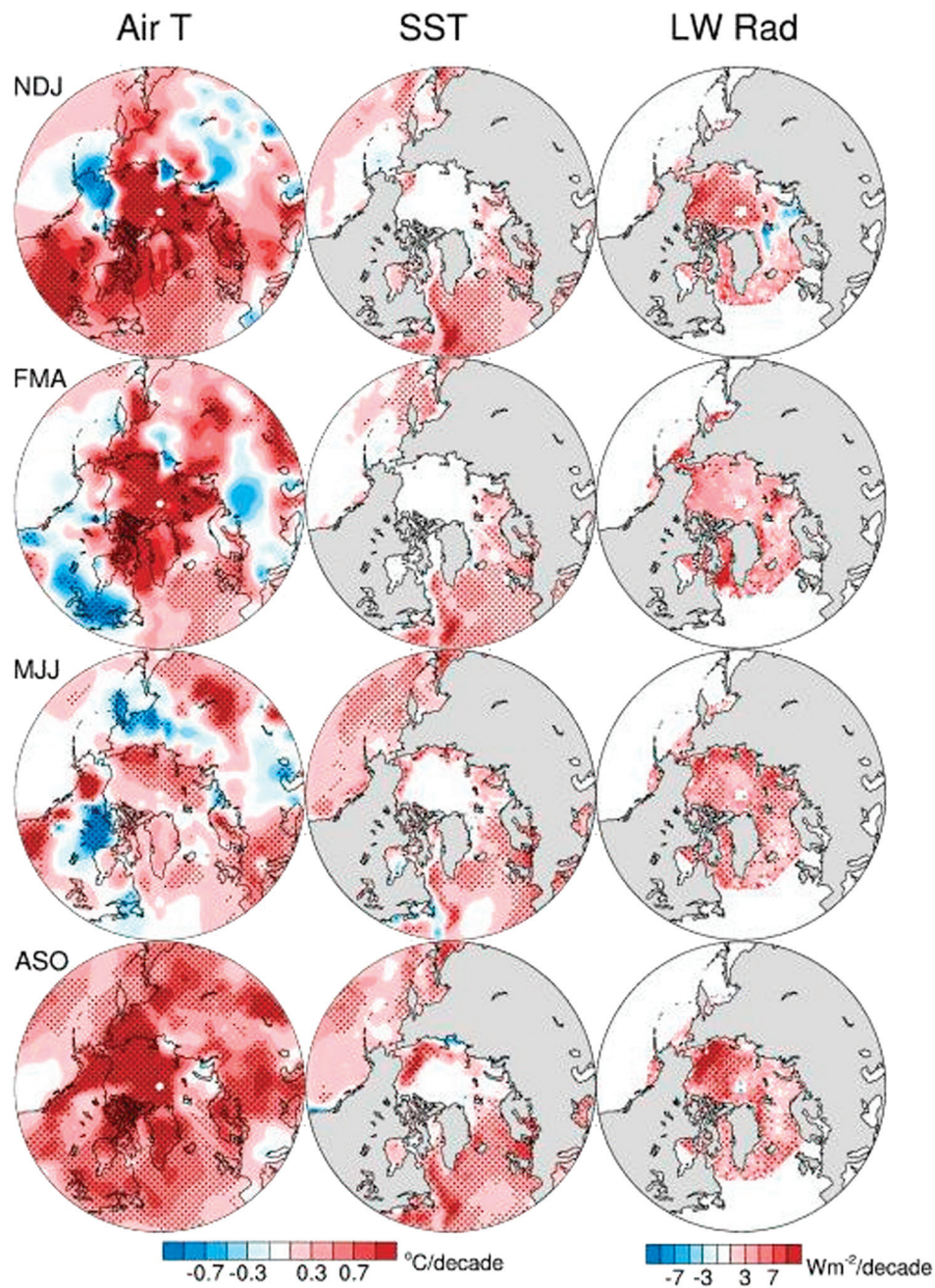


**Plate 7.** Trends in (left) 2-m air temperature ( $^{\circ}\text{C}$  per decade), (middle) sea surface temperature ( $^{\circ}\text{C}$  per decade), and (right) net surface downward longwave radiation ( $\text{W m}^{-2}$  per decade) during 1979–2007 for each season as indicated. Stippling indicates trend values statistically significant at the 95% level. Note that data after April 2007 are excluded from the trend calculations (the last month of data for longwave radiation is December 2005). Note that the coverage of the longwave radiation data is limited to north of  $55^{\circ}\text{N}$ .

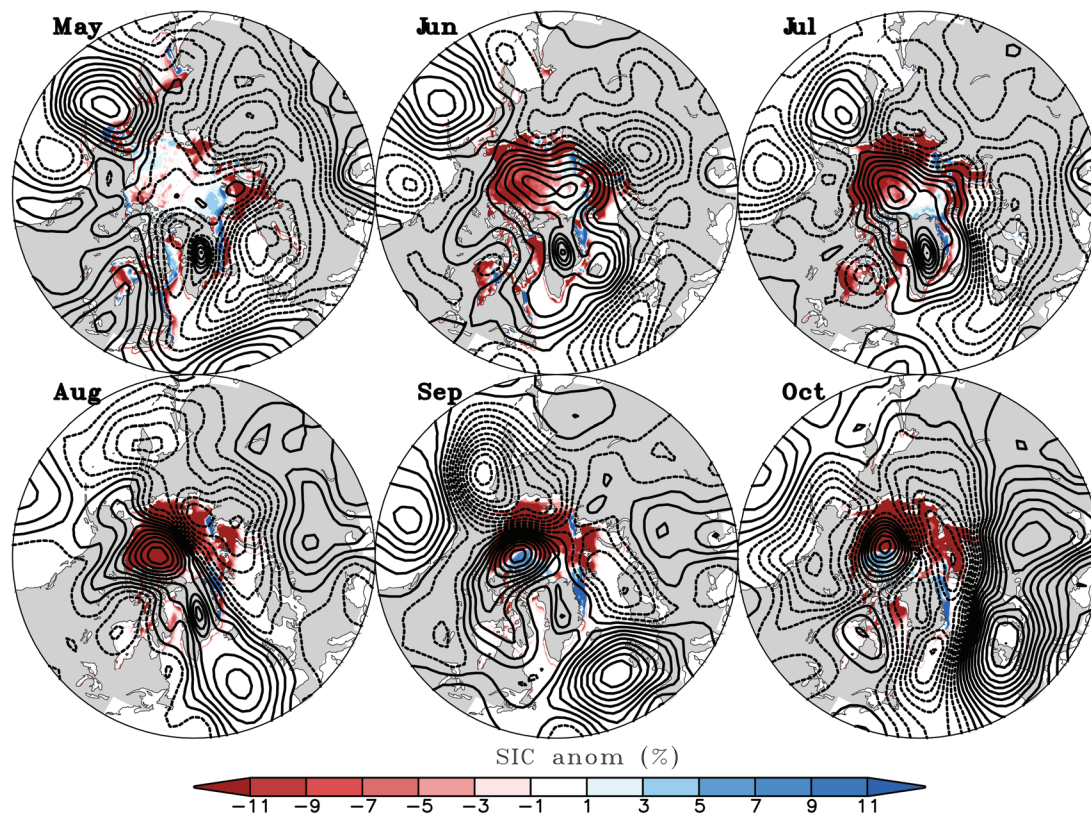


**Plate 8.** Monthly SLP (contours, hPa) and SIC (color shading, percent) anomaly maps for May through October 2007. The contour interval is 1 hPa; with negative values are dashed, and the zero and positive values are solid. Anomalies are defined relative to the 1979–2007 long-term monthly means.

these warming trends provide favorable environmental conditions for Arctic-wide sea ice losses since 1979, coupled with positive ice-albedo feedback and sea ice thinning.

*3.2.4. SIC and SLP anomaly maps for spring/summer 2007.* The drastic reduction of Arctic sea ice extent during the summer of 2007 deserves additional mention. Plate 8 shows the monthly SLP and SIC anomaly maps from May 2007 through October 2007, where anomalies are defined relative to the 1979–2006 long-term monthly means. Similar maps were presented by *Comiso et al.* [2008]. Large SIC losses within the central Arctic developed in June and reached peak amplitudes from late August to early September, leaving much of the eastern Arctic Ocean ice free [see also *Stroeve et al.*, 2008]. The SLP field was highly anomalous in all months of reduced SIC, featuring persistent high-pressure anomalies over the central Arctic Ocean and low-pressure anomalies over Eurasia and adjacent seas: this pattern resembles the distribution summer SLP trends during 1993–2007 (recall Plate 5). This configuration of SLP anomalies resulted in large geostrophic easterly wind anomalies over the marginal ice zone in June and July and strong southerly wind anomalies over the Beaufort, Chukchi, and East Siberian seas in August through October where the largest SIC losses were observed. It is likely that the low-level wind anomalies contributed to the massive sea ice reductions during summer 2007, a point also made by *Slingo and Sutton* [2007]. Reduced cloudiness and associated enhancement of downwelling shortwave radiation also played an important role [*Kay et al.*, 2008].

We note that the role of atmospheric circulation forcing of the 2007 summer SIC anomalies does not negate our conclusion that the overall retreat of Arctic sea ice since 1979 is not directly controlled by long-term atmospheric circulation changes. Indeed, we expect that atmospheric circulation anomalies will continue to play an important role in individual years, especially as the ice pack continues to thin, but that over the long term they become less important compared to other factors such as the positive ice-albedo feedback mechanism and greenhouse gas-induced warming of the atmosphere and ocean.

#### 4. SUMMARY AND DISCUSSION

The purpose of this study was to document aspects of the evolving trends in Arctic sea ice extent and concentration during 1979–2007 and to place them within the context of overlying changes in the atmospheric circulation. In addition to examining trends over the period as a whole, we investigated trends over the two halves of the record separately as a simple way of characterizing their evolution. It was

noted that the first half coincides with an upward trend in the NAM, the leading pattern of winter atmospheric circulation variability over the extratropical Northern Hemisphere that is known to exert a strong influence on Arctic sea ice cover, while the second half coincides with a downward trend in the NAM. We used 5-day running mean sea ice concentration data on a 25 km × 25 km grid derived from passive microwave measurements from 1 January 1979 through 31 October 2007.

Our main findings are as follows. Arctic sea ice extent has been retreating throughout the year, with the largest declines occurring from mid July to mid October. Overall, the pace of retreat as estimated from linear least squares regression analysis is  $-0.52 \times 10^6$  km<sup>2</sup> per decade ( $\sim -5\%$  of the mean per decade) or  $-1.76 \times 10^6$  km<sup>2</sup> in total during 1979–2007. The rate of retreat has accelerated from  $-0.35 \times 10^6$  km<sup>2</sup> per decade in the first half of the record (1979–1993) to  $-0.9 \times 10^6$  km<sup>2</sup> per decade in the second half of the record (1993–2007). The date of maximum (minimum) sea ice extent has increased by approximately 4 (1) days per decade, equivalent to a delay of approximately 10 (3) days in 2007 compared to 1979. The number of days with sea ice concentrations less than 50% over the Arctic as a whole has increased by 19 days from 1979 to 2007.

In each season, the spatial patterns of the SIC trends in the two halves of the record are distinctive. The first half is characterized by regional trends of opposing sign, and the second half is characterized by uniformly negative trends that resemble those over the full period. These distinctive trend patterns correspond in each season to the first two leading EOFs of SIC anomalies during 1979–2007. In spring, summer, and autumn, the leading (second) EOF corresponds to the trend pattern over the full record (first half), while in winter the order of the EOFs is reversed.

SIC trends in the first half of the record are characterized by positive values in the sub-Arctic seas of the western Atlantic and eastern Pacific and negative values in the peripheral seas of the eastern Atlantic and western Pacific in autumn, winter, and spring. In summer, the first half of the record exhibits positive SIC trends in the eastern Atlantic (Greenland and Barents seas) and negative trends in the Arctic (East Siberian, Chukchi, and eastern Beaufort seas). Atmospheric circulation trends, in particular a positive trend in the NAM, contributed to forcing the SIC trends in the first half of the record in all seasons via wind-induced low-level atmospheric thermal advection. In the second half of the record, the SIC declines in the Labrador, Barents, Kara, and Bering seas in fall and winter are associated with increased warm air advection in part because of a negative trend in the NAM. However, the pronounced SIC declines within the Arctic Ocean in spring and summer in the second half of the

study period are not accompanied by commensurately large positive trends in low-level thermal advection.

During the period 1979–2007 as a whole, atmospheric circulation trends and associated changes in wind-induced low-level thermal advection are weak in all seasons; as a result, they are unlikely to have played a dominant role in the overall retreat of Arctic sea ice since 1979. However, Arctic air temperatures, SSTs, and net surface downward longwave radiation have all increased since 1979 and thus collectively provide a favorable environment for sea ice loss.

Our findings are in qualitative agreement with those of Francis and Hunter [2006, 2007], who examined some of the forcing factors for regional SIC variations in winter and summer. In particular, Francis and Hunter [2007] analyzed satellite-derived estimates of downwelling longwave radiation, low-level winds, and SSTs in relation to winter SIC variations in the Bering and Barents seas during 1979–2005. They found that wind anomalies were the dominant forcing mechanism in the Bering Sea, while a combination of wind and SST anomalies were the main factors in the Barents Sea. In a related paper, Francis and Hunter [2006] showed that downward longwave radiation was the primary cause of summer sea ice extent variations during 1979–2004 throughout the Arctic marginal ice zone. They also reported that wind anomalies played a role in forcing summer sea ice extent anomalies in the Barents and Chukchi seas before, but not after, 1991. The results shown here based on SLP and wind-induced atmospheric thermal advection trends are in general agreement with the findings of Francis and Hunter [2006, 2007], although we note that a direct comparison is not possible because of the different timescales of variability examined in the two studies (interannual and longer in the case of Francis and Hunter and trends in our case).

In summary, our results lend additional support to the findings of numerous studies that factors other than long-term atmospheric circulation trends are playing a dominant role in the overall retreat of Arctic sea ice since 1979. These include warming of the upper ocean [Polyakov *et al.*, 2005; Shimada *et al.*, 2006; Stroeve and Maslowski, 2008; Steele *et al.*, 2008] and lower atmosphere [Comiso, 2003; Serreze *et al.*, 2007; Comiso *et al.*, 2008], sea ice thinning and associated reduction in multiyear ice fraction [Kwok, 2007; Rothrock *et al.*, 2007; Nghiem *et al.*, 2007], increased oceanic absorption of solar radiation in summer associated with the mechanism of positive ice-albedo feedback [Perovich *et al.*, 2007] and enhanced downwelling longwave radiative flux due to increased water vapor, cloudiness and carbon dioxide concentration [Francis and Hunter, 2006, 2007]. A better understanding of these and other processes affecting Arctic sea ice remains an important task with relevance to future predictions of Arctic climate change.

*Acknowledgments.* We thank the two anonymous reviewers and Editor Eric DeWeaver for constructive suggestions. We are grateful to the National Snow and Ice Data Center for providing the sea ice concentration data. Clara Deser acknowledges support from the NSF Office of Polar Programs (ARCSS), and Haiyan Teng acknowledges support from the U.S. Department of Energy under Cooperative Agreement DE-FC02-97ER62402. The National Center for Atmospheric Research is sponsored by the National Science Foundation.

## REFERENCES

- Cavalieri, D. J., C. L. Parkinson, P. Gloersen, J. C. Comiso, and H. J. Zwally (1999), Deriving long-term time series of sea ice cover from satellite passive-microwave multisensor data sets, *J. Geophys. Res.*, *104*, 15,803–15,814.
- Comiso, J. C. (2003), Arctic warming signals from clear-sky surface temperature satellite observations, *J. Clim.*, *16*, 3498–3510.
- Comiso, J. C. (2006), Abrupt decline in the Arctic winter sea ice cover, *Geophys. Res. Lett.*, *33*, L18504, doi:10.1029/2006GL027341.
- Comiso, J. C., C. L. Parkinson, R. Gersten, and L. Stock (2008), Accelerated decline in the Arctic sea ice cover, *Geophys. Res. Lett.*, *35*, L01703, doi:10.1029/2007GL031972.
- Deser, C. (2000), On the teleconnectivity of the “Arctic Oscillation,” *Geophys. Res. Lett.*, *27*, 779–782.
- Deser, C., and H. Teng (2008), Evolution of Arctic sea ice concentration trends and the role of atmospheric circulation forcing, 1979–2007, *Geophys. Res. Lett.*, *35*, L02504, doi:10.1029/2007GL032023.
- Deser, C., J. E. Walsh, and M. S. Timlin (2000), Arctic sea ice variability in the context of recent atmospheric circulation trends, *J. Clim.*, *13*, 617–633.
- Fang, Z., and J. M. Wallace (1994), Arctic sea ice variability on a timescale of weeks: Its relation to atmospheric forcing, *J. Clim.*, *7*, 1897–1913.
- Francis, J. A., and E. Hunter (2006), New insight into the disappearing Arctic sea ice, *Eos Trans. AGU*, *87*(46), 509, doi:10.1029/2006EO460001.
- Francis, J. A., and E. Hunter (2007), Drivers of declining sea ice in the Arctic winter: A tale of two seas, *Geophys. Res. Lett.*, *34*, L17503, doi:10.1029/2007GL030995.
- Holland, M. M., C. M. Bitz, and B. Tremblay (2006), Future abrupt reductions in the summer Arctic sea ice, *Geophys. Res. Lett.*, *33*, L23503, doi:10.1029/2006GL028024.
- Hu, A., C. Rooth, R. Bleck, and C. Deser (2002), NAO influence on sea ice extent in the Eurasian coastal region, *Geophys. Res. Lett.*, *29*(22), 2053, doi:10.1029/2001GL014293.
- Hurrell, J. W. (1995), Decadal trends in the North Atlantic Oscillation: Regional temperatures and precipitation, *Science*, *269*, 676–679.
- Kalnay, E., et al. (1996), The NCEP/NCAR 40-year reanalysis project, *Bull. Am. Meteorol. Soc.*, *77*, 437–471.
- Kay, J. E., T. L’Ecuyer, A. Gettelman, G. Stephens, and C. O’Dell (2008), The contribution of cloud and radiation anomalies to the

- 2007 Arctic sea ice extent minimum, *Geophys. Res. Lett.*, *35*, L08503, doi:10.1029/2008GL033451.
- Kwok, R. (2007), Near zero replenishment of the Arctic multiyear sea ice cover at the end of 2005 summer, *Geophys. Res. Lett.*, *34*, L05501, doi:10.1029/2006GL028737.
- Lindsay, R. W., and J. Zhang (2005), The thinning of Arctic sea ice, 1988–2003: Have we reached the tipping point?, *J. Clim.*, *18*, 4879–4895.
- Maslanik, J., S. Drobot, C. Fowler, W. Emery, and R. Barry (2007), On the Arctic climate paradox and the continuing role of atmospheric circulation in affecting sea ice conditions, *Geophys. Res. Lett.*, *34*, L03711, doi:10.1029/2006GL028269.
- Meier, W. N., J. Stroeve, and F. Fetterer (2007), Whither Arctic sea ice?: A clear signal of decline regionally, seasonally and extending beyond the satellite record, *Ann. Glaciol.*, *46*, 428–434.
- Nghiem, S. V., I. G. Rigor, D. K. Perovich, P. Clemente-Colón, J. W. Weatherly, and G. Neumann (2007), Rapid reduction of Arctic perennial sea ice, *Geophys. Res. Lett.*, *34*, L19504, doi:10.1029/2007GL031138.
- North, G. R., T. L. Bell, R. F. Calahan, and F. J. Moeng (1982), Sampling errors in the estimation of empirical orthogonal functions, *Mon. Weather Rev.*, *110*, 699–706.
- Overland, J. E., and M. Wang (2005), The Arctic climate paradox: The recent decrease of the Arctic Oscillation, *Geophys. Res. Lett.*, *32*, L06701, doi:10.1029/2004GL021752.
- Perovich, D. K., B. Light, H. Eicken, K. F. Jones, K. Runciman, and S. V. Nghiem (2007), Increasing solar heating of the Arctic Ocean and adjacent seas, 1979–2005: Attribution and role in the ice-albedo feedback, *Geophys. Res. Lett.*, *34*, L19505, doi:10.1029/2007GL031480.
- Polyakov, I. V., et al. (2003), Long-term ice variability in Arctic marginal seas, *J. Clim.*, *16*, 2078–2085.
- Polyakov, I. V., U. S. Bhatt, R. Colony, D. Walsh, G. V. Alekseev, R. V. Bekryaev, V. P. Karklin, A. V. Yulin, and M. A. Johnson (2005), One more step toward a warmer Arctic, *Geophys. Res. Lett.*, *32*, L17605, doi:10.1029/2005GL023740.
- Portis, D. H., J. E. Walsh, M. El Hamly, and P. J. Lamb (2001), Seasonality of the North Atlantic Oscillation, *J. Clim.*, *14*, 2069–2078.
- Rayner, N. A., D. E. Parker, E. B. Horton, C. K. Folland, L. V. Alexander, D. P. Rowell, E. C. Kent, and A. Kaplan (2003), Global analyses of sea surface temperature, sea ice, and night marine air temperature since the late nineteenth century, *J. Geophys. Res.*, *108*(D14), 4407, doi:10.1029/2002JD002670.
- Rigor, I. G., and J. M. Wallace (2004), Variations in the age of Arctic sea-ice and summer sea-ice extent, *Geophys. Res. Lett.*, *31*, L09401, doi:10.1029/2004GL019492.
- Rigor, I. G., J. M. Wallace, and R. L. Colony (2002), Response of sea ice to the Arctic Oscillation, *J. Clim.*, *15*, 2648–2663.
- Rothrock, D. A., and J. Zhang (2005), Arctic Ocean sea ice volume: What explains its recent depletion?, *J. Geophys. Res.*, *110*, C01002, doi:10.1029/2004JC002282.
- Rothrock, D. A., D. B. Percival, and M. Wensnahan (2008), The decline in Arctic sea-ice thickness: Separating the spatial, annual, and interannual variability in a quarter century of submarine data, *J. Geophys. Res.*, *113*, C05003, doi:10.1029/2007JC004252.
- Serreze, M. C., and J. A. Francis (2006), The Arctic amplification debate, *Clim. Change*, *76*, 241–264, doi:10.1007/s10584-005-9017-y.
- Serreze, M. C., M. M. Holland, and J. Stroeve (2007), Perspectives on the Arctic's shrinking sea-ice cover, *Science*, *315*, 1533–1536.
- Shimada, K., T. Kamoshida, M. Itoh, S. Nishino, E. Carmack, F. A. McLaughlin, S. Zimmermann, and A. Proshutinsky (2006), Pacific Ocean inflow: Influence on catastrophic reduction of sea ice cover in the Arctic Ocean, *Geophys. Res. Lett.*, *33*, L08605, doi:10.1029/2005GL025624.
- Slingo, J., and R. Sutton (2007), Sea-ice decline due to more than warming alone, *Nature*, *450*, 27.
- Steele, M., W. Ermold, and J. Zhang (2008), Arctic Ocean surface warming trends over the past 100 years, *Geophys. Res. Lett.*, *35*, L02614, doi:10.1029/2007GL031651.
- Stroeve, J., and W. Maslowski (2008), Arctic sea ice variability during the last half century, in *Climate Variability and Extremes During the Past 100 Years*, *Adv. Global Change Res.*, vol. 33, pp. 143–154, Springer, New York.
- Stroeve, J., T. Markus, W. Meier, and J. Miller (2006), Recent changes in the Arctic melt season, *Ann. Glaciol.*, *44*, 367–374.
- Stroeve, J., M. M. Holland, W. Meier, T. Scambos, and M. Serreze (2007), Arctic sea ice decline: Faster than forecast, *Geophys. Res. Lett.*, *34*, L09501, doi:10.1029/2007GL029703.
- Stroeve, J., M. Serreze, S. Drobot, S. Gearheard, M. Holland, J. Maslanik, W. Meier, and T. Scambos (2008), Arctic sea ice extent plummets in 2007, *Eos Trans. AGU*, *89*(2), 13, doi:10.1029/2008EO020001.
- Thompson, D. W. J., and J. M. Wallace (2000), Annular modes in the extratropical circulation. Part I: Month-to-month variability, *J. Clim.*, *13*, 1000–1026.
- Ukita, J., M. Honda, H. Nakamura, Y. Tachibana, D. J. Cavalieri, C. L. Parkinson, H. Koide, and K. Yamamoto (2007), Northern Hemisphere sea ice variability: Lag structure and its implications, *Tellus, Ser. A*, *59*, 261–272, doi:10.1111/j.1600-0870.2006.00223.x.
- Walsh, J. E., and C. M. Johnson (1979), An analysis of Arctic sea ice fluctuations, 1953–1977, *J. Phys. Oceanogr.*, *9*, 580–591.

---

C. Deser and H. Teng, Climate and Global Dynamics Division, NCAR, P.O. Box 3000, Boulder, CO 80307, USA. (cdeser@ucar.edu)